Temperature Effect on Co-based Catalysts in Oxygen Evolution Reaction

*Guangxing Zhang+, Han Wang+, Jinlong Yang, Qinghe Zhao, Luyi Yang, Hanting Tang, Chaokun Liu, Haibiao Chen, Yuan Lin, and Feng Pan**

School of Advanced Materials, Shenzhen Graduate School, Peking University
Shenzhen 518055, People's Republic of China

Corresponding Author
**E-mail address:*panfeng@pkusz.edu.cn (F. Pan)

Experimental Sections

Materials and synthesis: IrO_2 powers were purchased from Alfa; Co_3O_4 nanorods were calcined from $Co(CO_3)_{0.35}Cl_{0.2}(OH)_{1.1}$ which was synthesized via hydrothermal method[1]. Li_2CoSiO_4 (LCS) nanoparticales were prepared through microwave-assisted hydrothermal synthesis.First, Lithium hydroxide (6 mmol), Cobalt sulfate (1.5 mmol) and ethylorthosilicate (1.5 mmol) were dissolved in 30 mL water/ethanol mixture (1/1 in volume). Then, the mixture was poured into a 100 mL Teflon-lined autoclave, sealed and microwave heated at 200℃ for 1 h. The final dark blue powders were centrifuged and washed with water and ethanol many times, and then dried at 70℃ over night. Amorphous FeCo(OH)x nanoflowers were potentiostatically electrodeposited onto the Ni foams in the three electrode system. The Ni foam and platinum were used as working electrode and counter electrode, respectively. The electrolyte contained ferrous nitrate (0.8 M) and cobalt nitrate (0.2 M) in 50 mL distilled water. The deposition was controlled at -1.0 V (vs. Ag/AgCl) for 10 mins.

Materials Characterization: X-ray diffraction (Bruker D8 Advance diffractometer with Cu Kα) was used to investigate the crystal structures of the samples. The micro-structures of the samples were characterized through scanning electron microscopy (FE-SEM, ZEISS Supra 55). The surface area and the pore size distribution were investigated through BET nitrogen adsorption/desorption (BET, Micromeritics ASAP 2020 HD88). XPS analyses were explored via an ESCALAB 250XL.

Electrochemistry: The electrochemical measurements were carried out with a CHI 660E at different temperature and the temperature was controlled through an oil bath device. The electrolyte was a 1 M KOH or 0.1 M KOH solution. In the three electrode system, a saturated Ag/AgCl electrode and platinum were used as the reference electrode and the counter electrode, respectively. The working electrode was a layer of catalyst casted onto Ni foam as detailed in the following: 0.1 g of catatlys, 0.1 g of ethyl cellulose ethoce and 0.8 g of terpineol were added into 4 mL ethanol. Then, the mixture was agitated overnight until it became viscous ink. Then the ink was dropped onto Ni foam (1×1 cm), and dried under lamp. Ni foam, as a current collector, possesses high conductivity and is benefit to decrease the contact resistance between catalyst and current collector. In addition, the multihole structures of Ni foam promotes the adsorption of the reactants molecules. LSV curves and Tafel slopes of Ni foam in Fig. S2 prove that Ni is really a pretty decent catalyst for the OER reaction. However, OER reaction is on the surface of the catalyst. XPS shows that for the Ni foam the binding energies of Ni 2p3/2 and Ni 2p1/2 locate at around 856 eV and 873 eV, respectively. While, for Co_3O_4@Ni foam electrode, both binding energies of Ni 2p3/2 and Ni 2p1/2 were lack, indicating that the Ni foam almost completely covered by Co_3O_4 catalyst. Furthermore, the Tafel slopes of Ni foam change linearly with the temperature, demonstrating that the Ni foam does not affect the rule of Co-based OER catalysts with temperature.

Calculation Method: The potential relative to reversible hydrogen electrode (E_{RHE}) with temperature is calculated according to the following Equations[2, 3]:

$$E_{RHE} = E_{applied} + E_{ref} + 2.303*RT*pH/F \quad (1)$$

$$pH=-lg(K_w/[OH^-]) \quad (2)$$

$E_{applied}$ means applied potential, the E_{ref} is potential of saturated Ag/AgCl reference electrode and calibrated with respect to temperature[4] (Fig. S3), R is ideal gas constant (8.314 $JK^{-1}mol^{-1}$), T is temperature (K). F is faraday constant (96485 $JV^{-1}mol^{-1}$) and n is electron transfer number, K_w is ionization constant of H_2O and calibrated with respect to temperature according to the following Equation (3)[5]:

$$\Delta G° = \Delta H° - \Delta S°T = -RT*\ln K_w \quad (3)$$

Where $\Delta G°$, $\Delta H°$ and $\Delta S°$ is the standard Gibbs free energy, enthalpy and entropy changes related to H_2O (l), respectively. The K_w values at different temperatures can be deduced by a linear relationship between the logarithm of K_w and the reciprocal of temperature (1/T), which is shown in Fig. S4. The overpotentials (η) at different temperatures are calculated according to following Equations[6]:

$$\eta = E_{RHE} - E_{H2O} \tag{4}$$

$$(\partial E/\partial T)_P = \Delta S/nF = [S_{H2O(l)} - S_{H2(g)} - 0.5 S_{O2(g)}]/2F = -0.842 mVK^{-1} \tag{5}$$

E_{H2O} is the theoretical decomposition potential of water, and the value is 1.23 V at 25℃, $(\partial E/\partial T)_P$ is the temperature coefficient of E_{H2O} at 0.1MP.

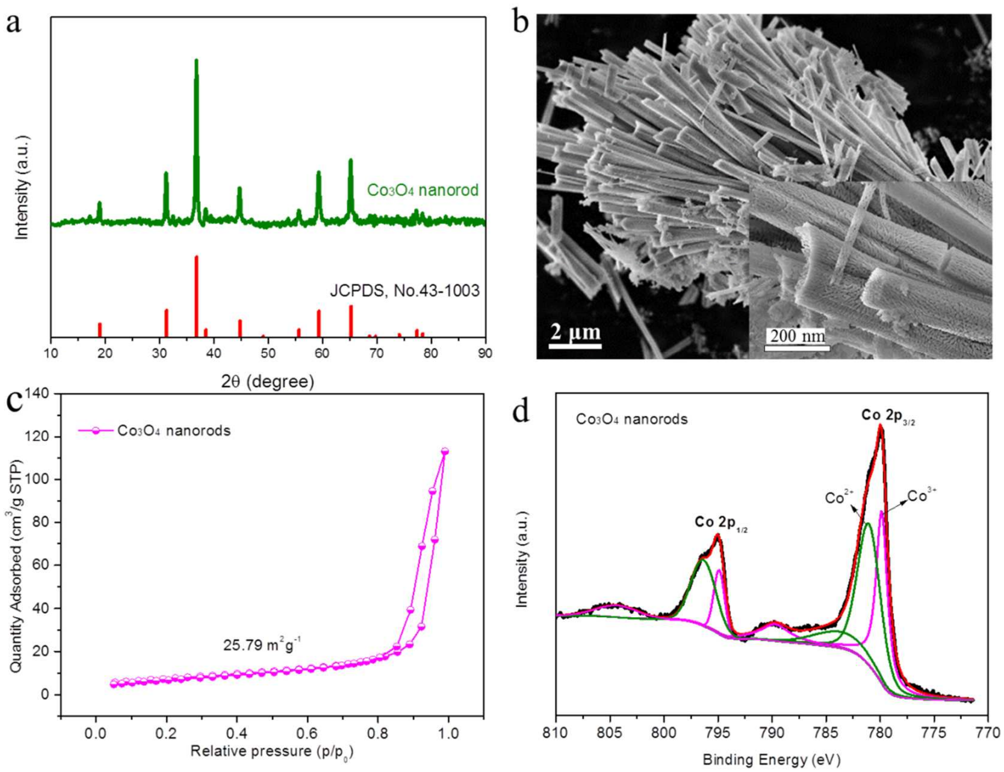

Figure S1 (a) XRD pattern (b) SEM images (c) BET and (d) XPS of Co_3O_4 catalyst.

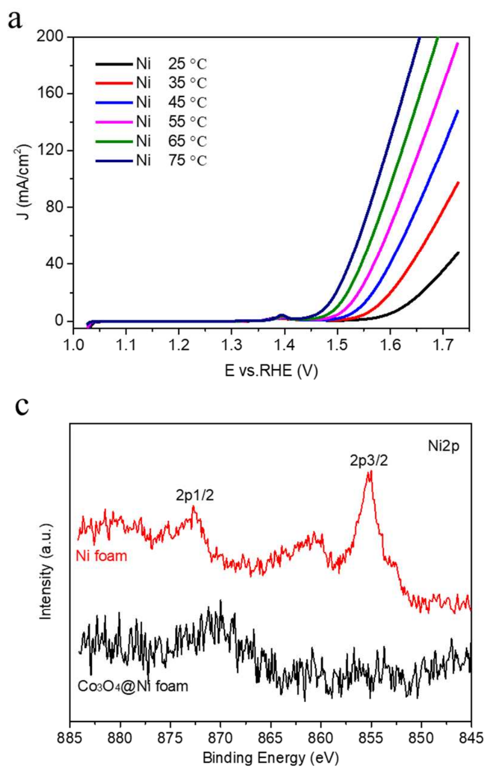

Figure S2 (a) LSV curves at 2 mV s^{-1} and (b) Tafel plots for Ni foam in 1M KOH at temperature from 25□ to 75□, (c) Ni 2p binding energies and (d) Tafel slope plotted against temperature (T) of Ni foam and catalysts on Ni foam.

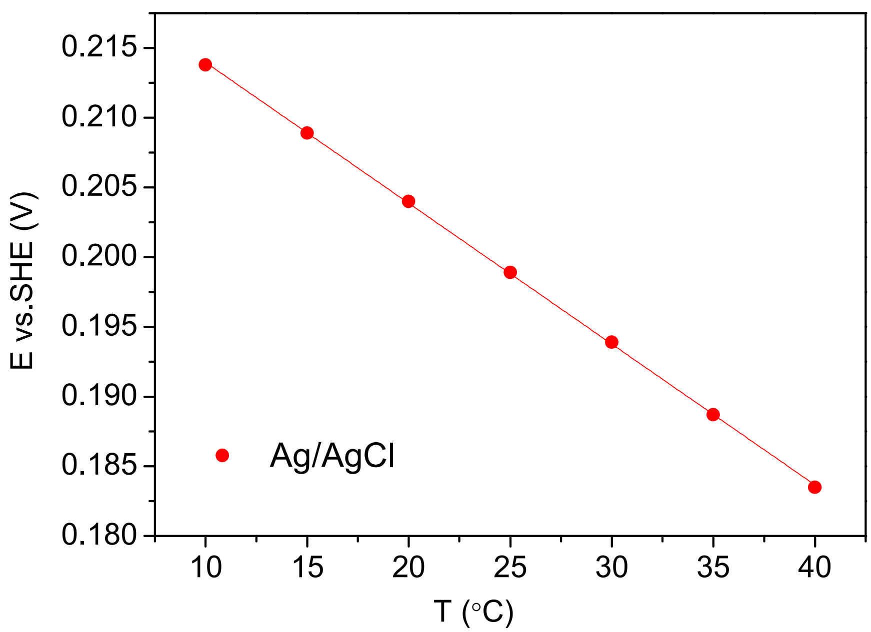

Figure S3 the liner relationship of the potential of saturated Ag/AgCl reference electrode with temperature.

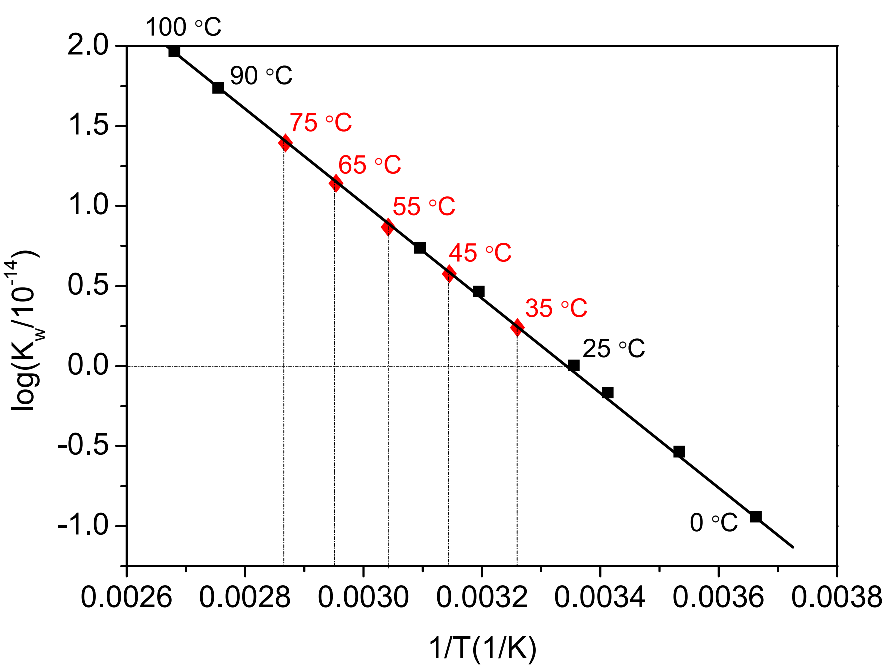

Figure S4 linear relationship between the logarithm of K_w and the reciprocal of temperature (1/T).

Table S1 Comparison of Tafel slope at room temperature for reported Co_3O_4.

Co_3O_4 Catalysts	Tafel slope (mV dec^{-1})	Electrolyte	Ref.
Co_3O_4 Nanorod	**111**	**1 M KOH**	**This work**
Co_3O_4 nanowire arrays	112	1 M KOH	Angew , 2016, 55, 1
Zn doped Co_3O_4	113	1 M KOH	JACS, 2016, 138 ,36
Co_3O_4 nanocages	110	1 M KOH	JACS, 2015, 137, 5590
Meso-Co_3O_4 Nanowire	72	1 M KOH	AEM, 2014, 4, 1400696
Co_3O_4 Nanocube	95	1 M KOH	ACS AMI, 2015, 7, 442
Co_3O_4 nanocrystal	161	1 M KOH	CC, 2015, 51, 8066
rGO- Co_3O_4 Yolk-Shell	101	1 M KOH	JMCA, 2016, 4, 13534
Co_3O_4/N-rmGO	67	1 M KOH	Nat. Mater. 2011, 10, 780
Ni doped Co_3O_4	292	1 M KOH	JPCC, 2014, 118, 25939

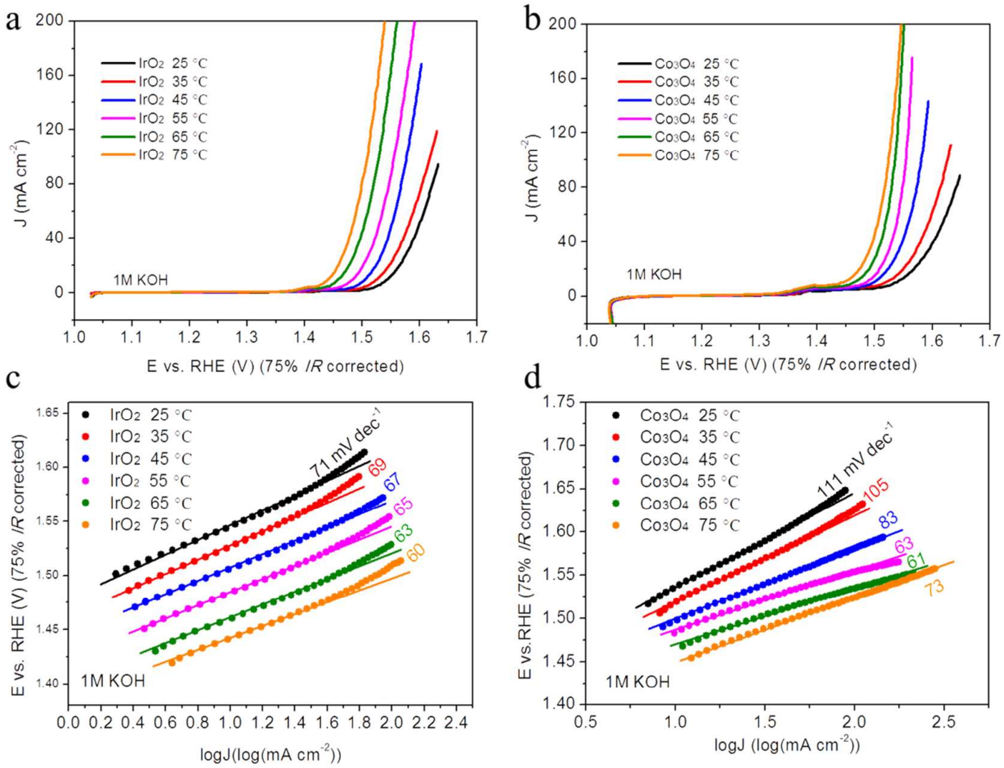

Figure S5 (a, c) LSV curvesat 2 mV s^{-1}and (b, d) Tafel plots with reference to Reversible Hydrogen Electrode (E_{RHE}) and 75% IR correction for (a, b) IrO_2 and (c, d) Co_3O_4 catalysts in 1M KOH at room temperature from 25℃to 75℃.

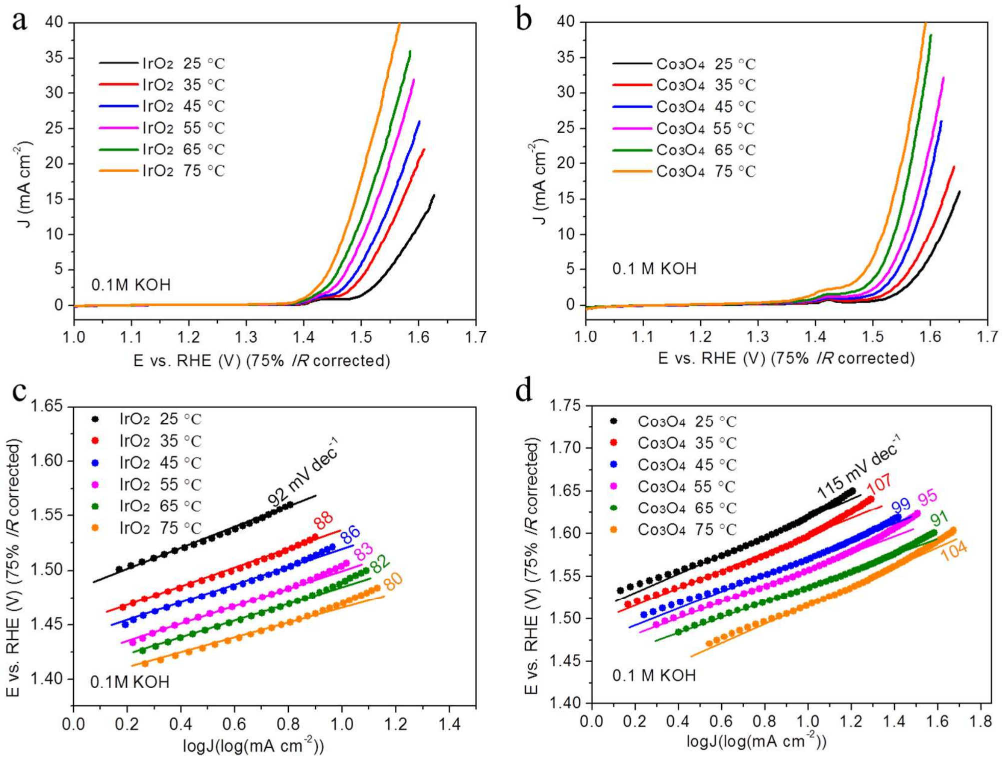

Figure S6 (a, c) LSV curves at 2 mV $s^{-1}$and (b, d) Tafel plots with reference to Reversible Hydrogen Electrode (E_{RHE}) and 75% IR correction for (a, b) IrO_2 and (c, d) Co_3O_4 catalysts in 0.1M KOHat room temperature from 25℃to 75℃.

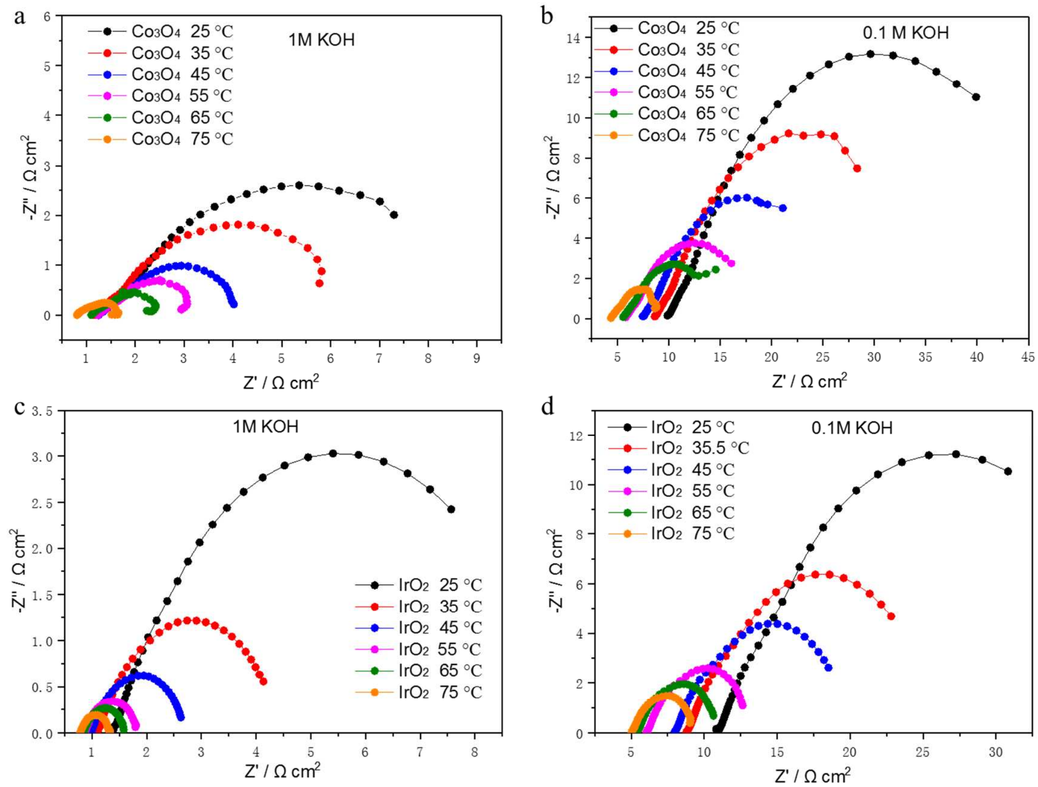

Figure S7 Nyquist plots for the Co_3O_4 catalysts measured at 1.5 V vs. RHE in 1M KOH (a) and in 0.1M KOH (b); IrO_2 in 1M KOH (c) and in 0.1M KOH (d).

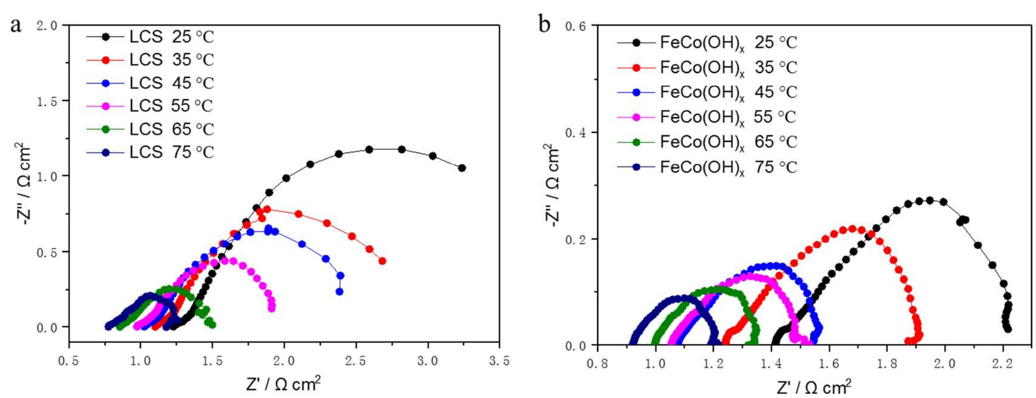

Figure S8 Nyquist plots for the LCS catalysts (a) and FeCo(OH)x (b) measured at 1.5 V vs. RHE in 1M KOH.

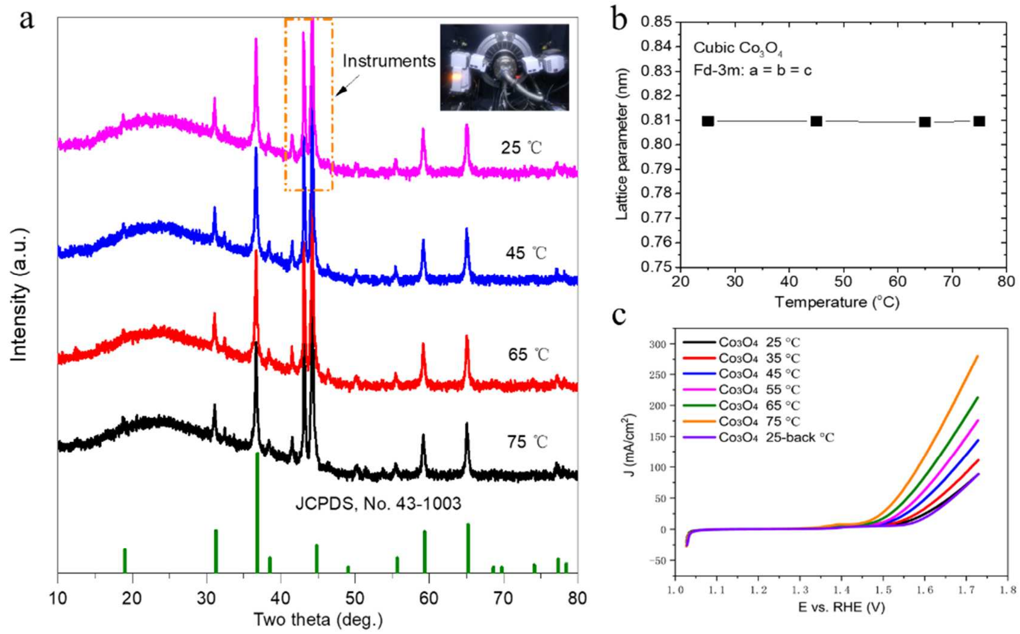

Figure S9 (a) In-situ XRD, (b) lattice parameters vs. temperatures for Co_3O_4 and (c) LSV curves at 2 mV s^{-1} for cubic Co_3O_4.

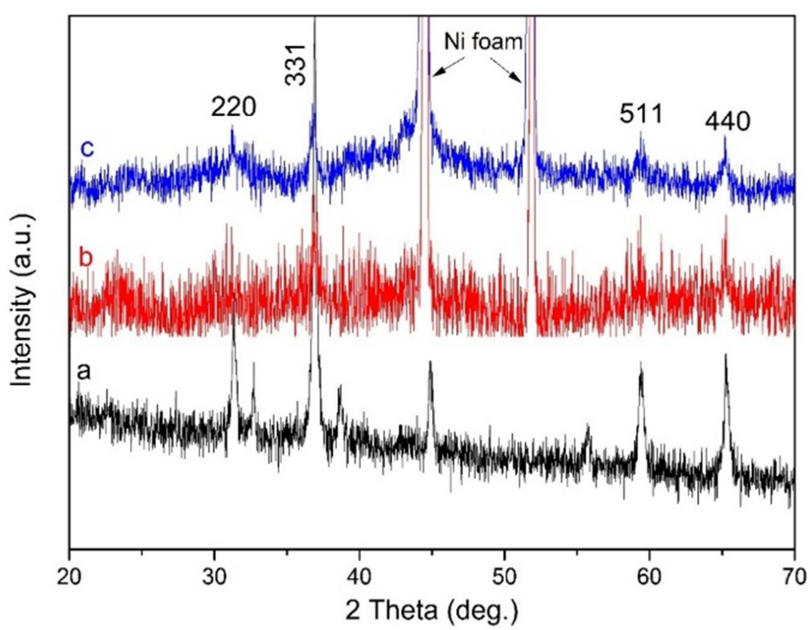

Figure S10 XRD of Co_3O_4 samples. (a) pristine Co_3O_4, (b) Co_3O_4 after OER performance at 25℃, (c) Co_3O_4 after OER performance at 65℃.

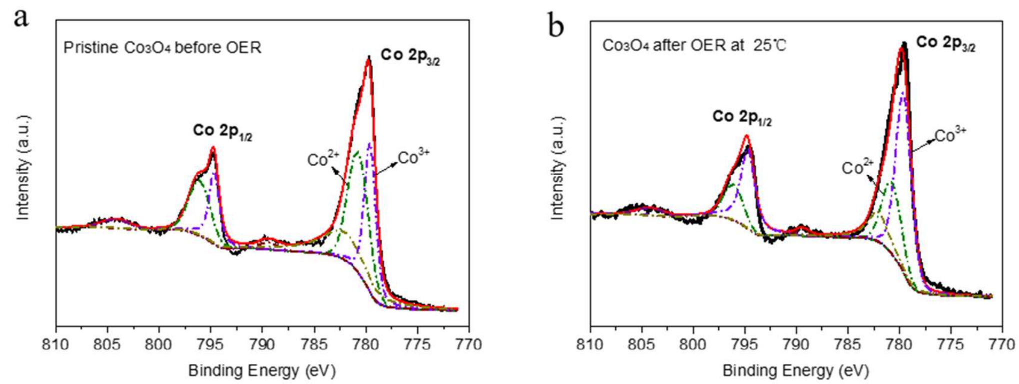

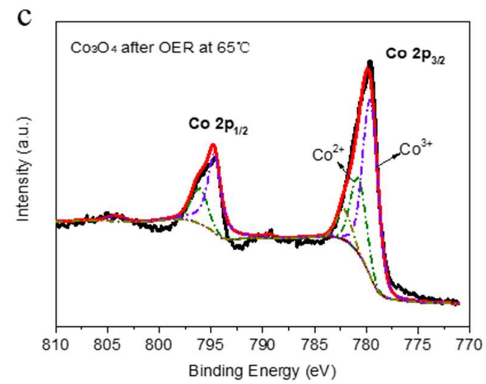

d

Co_3O_4	Co^{2+}/Co^{3+}
Before OER	1.23
After OER at 25°C	0.43
After OER at 65°C	0.42

Figure S11 Fitting Co2p for (a) pristine Co_3O_4, (b) Co_3O_4 after OER at 25□, (c) Co_3O_4 after OER at 65□; (d) the ratio of Co^{2+}/Co^{3+} in different samples.

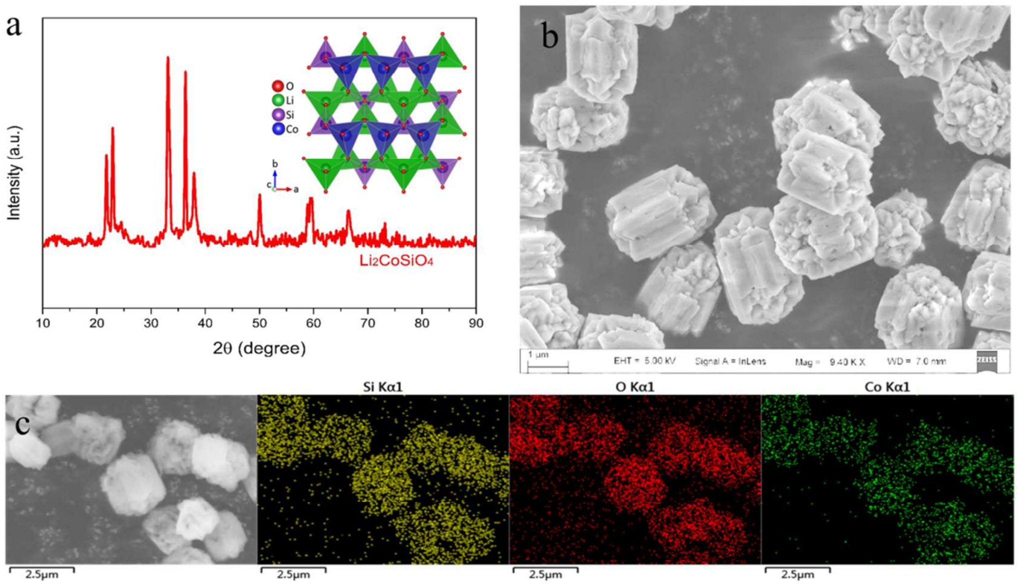

Figure S12 (a) XRD pattern, (b) SEM image and (c) EDX mapping of Li_2CoSiO_4 (LCS) catalyst.

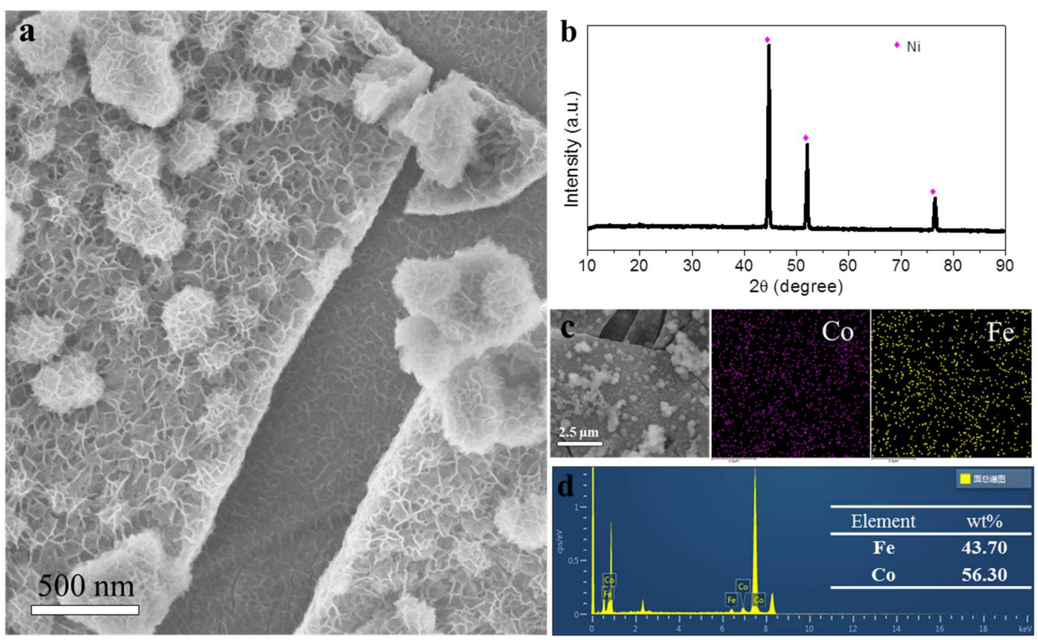

Figure S13 (a) SEM image, (b) XRD pattern and (c) EDX mapping and (d) ratio of Fe/Co of amorphous FeCo(OH)x grown on Ni foam.

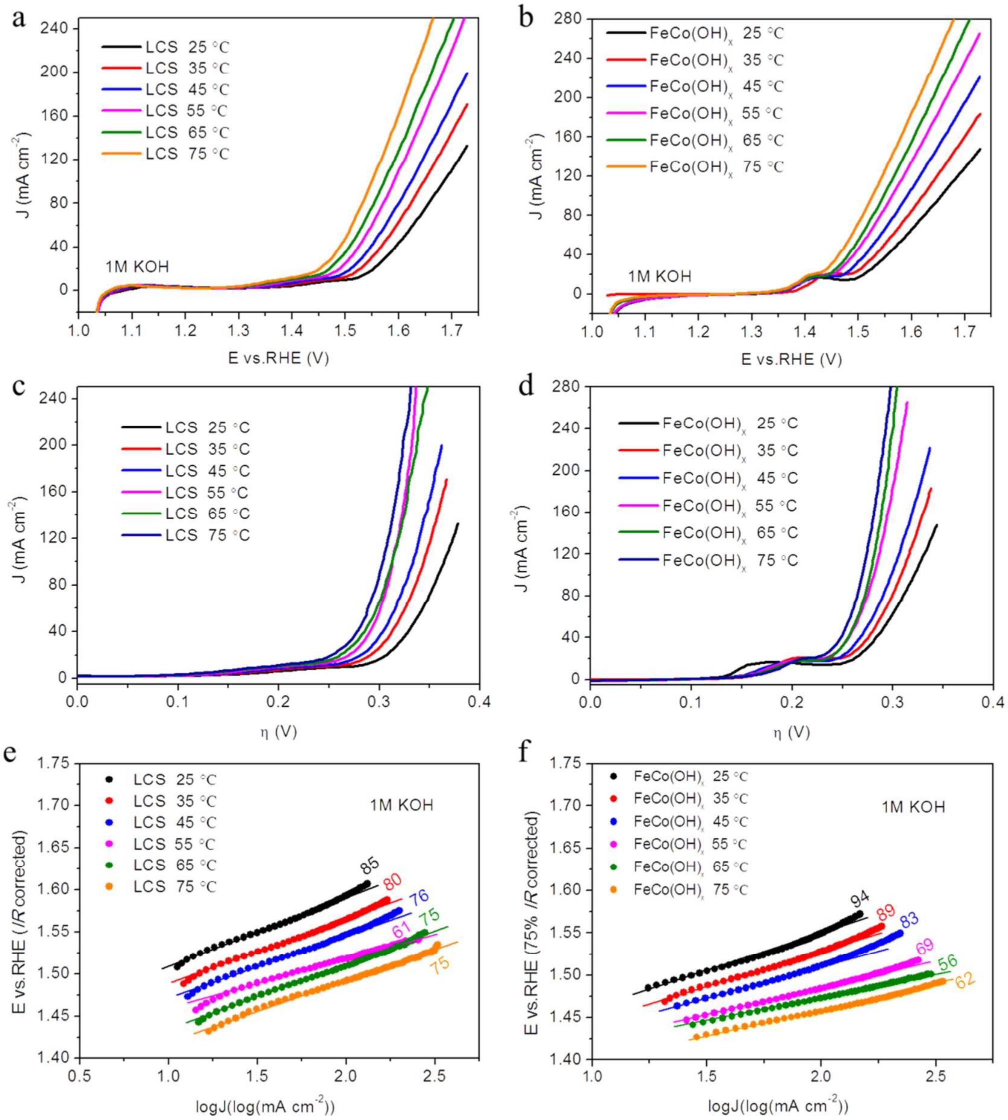

Figure S14 (a, b) Tested LSV curves at 2 mV s^{-1}, (c, d) calculated overpotentials and (e, f) Tafel plots for (a, c, e) LCS and (b, d, f) FeCo(OH)x catalysts in 1M KOH at temperature from 25℃ to 75℃.

References

[1] Wang, Y.; Zhou, T.; Jiang, K.; Da, P.; Peng, Z.; Tang, J.; Kong, B.; Cai, W. B.; Yang, Z.; Zheng, G. Reduced Mesoporous Co_3O_4 Nanowires as Efficient Water Oxidation Electrocatalysts and Supercapacitor Electrodes. *Adv. Energy Mater.* **2014**, *4*, 1400696.

[2] Li, Y.; Zhou, W.; Wang, H.; Xie, L.; Liang, Y.; Wei, F.; Idrobo, J. C.; Pennycook, S. J.; Dai, H. An Oxygen Reduction Electrocatalyst Based on Carbon Nanotube-Graphene Complexes. *Nat. Nanotechnol*. **2012**, *7*, 394-400.

[3] Li, Y.; Wang, H.; Xie, L.; Liang, Y.; Hong, G.; Dai, H. MoS_2 Nanoparticles Grown on Graphene: An Advanced Catalyst for the Hydrogen Evolution Reaction. *J. Am. Chem. Soc.* **2011**, *133*, 7296-7299.

[4] Shinagawa, T.; Ng, M. T.; Takanabe, K. Boosting the Performance of the Nickel Anode in the Oxygen Evolution Reaction by Simple Electrochemical Activation. *Angew. Chem. Int. Ed*. **2017**, *56*, 5061-5065.

[5] Clever, H. L. The Ion Product Constant of Water: Thermodynamics of Water Ionization. *J. Chem. Educ*, **1968**, *45*, 231-235.

[6] Macdonald, G. J. F. Gibbs Free Energy of Water at Elevated Temperatures and Pressures with Applications to the Brucite-Periclase Equilibrium. *J. Geology*, **1955**, *63*, 244-252.